

Synthesis and Characterization of Three-Coordinate and Related β -Diketimate Derivatives of Manganese, Iron, and Cobalt

Arunashree Panda,[†] Matthias Stender,[†] Robert J. Wright,[†] Marilyn M. Olmstead,[†] Peter Klavins,[‡] and Philip P. Power^{*†}

Departments of Chemistry and Physics, University of California, Davis, One Shields Avenue, Davis, California 95616

Received February 20, 2002

Treatment of $M\{N(SiMe_3)_2\}_2$ ($M = Mn, Fe, Co$) with various bulky β -diketamines afforded a variety of new three-coordinate complexes which were characterized by UV–vis, 1H NMR and IR spectroscopy, magnetic measurements, and X-ray crystallography. Reaction of the β -diketamine $H(Dipp)NC(Me)CHC(Me)N(Dipp)$ ($Dipp_2N^{\wedge}NH$; $Dipp = C_6H_3-2,6-Pr_2$) with $M\{N(SiMe_3)_2\}_2$ ($M = Mn$ or Co) gave $Dipp_2N^{\wedge}NMN(SiMe_3)_2$ ($M = Mn$, **1**; Co , **3**) while the reaction of $Fe\{N(SiMe_3)_2\}_2$ with $Ar_2N^{\wedge}NH$ ($Ar = Dipp, C_6F_5, Mes, C_6H_3-2,6-Me_2, \text{ or } C_6H_3-2,6-Cl_2$) afforded the series of iron complexes $Ar_2N^{\wedge}NFe\{N(SiMe_3)_2\}$ ($Ar = Dipp$, **2a**; C_6F_5 , **2b**; Mes , **2c**; $C_6H_3-2,6-Me_2$, **2d**; $C_6H_3-2,6-Cl_2$, **2e**). This represents a new synthetic route to β -diketimate complexes of these metals. The four-coordinate bis- β -diketimate complex $Fe\{N^{\wedge}N(C_6F_5)_2\}_2$, **4**, was also isolated as a byproduct from the synthesis of **2b**. Direct reaction of the $Dipp_2N^{\wedge}NLi$ with $CoCl_2$ gave the "ate" salt $Dipp_2N^{\wedge}NCoCl_2Li(THF)_2$, **5**, in which the lithium chloride has formed a complex with $Dipp_2N^{\wedge}NCoCl$ through chloride bridging. The $Fe(III)$ species $Dipp_2N^{\wedge}NFeCl_2$, **6**, was obtained cleanly from the reaction of $FeCl_3$ with $Dipp_2N^{\wedge}NLi$. Magnetic measurements showed that all the complexes have a high spin configuration. The different substituents in the series of iron complexes **2a–e** allowed assignment of their paramagnetically shifted 1H NMR spectra. The X-ray crystal structures **1–2d** and **3** showed that they have a distorted three-coordinate planar configuration at the metals whereas complexes **4–6** have highly distorted four-coordinate geometries.

Introduction

The divalent transition metal silylamides $M\{N(SiMe_3)_2\}_2$ ($M = Mn$,¹ Fe ,² or Co ³) are useful hydrocarbon soluble sources of M^{2+} that have semipolar and reactive $M-N$ bonds. They possess two-coordinate monomeric structures in the vapor phase² but exist as amide bridged dimers in the crystalline state.^{4–6} In solution, at room temperature, they are essentially dissociated to monomers but are weakly associated at low temperatures in an entropy driven equi-

librium.^{6,7} Their monomeric, coordinatively unsaturated structures confer high reactivity, and their chemistry has been dominated by reactions with Lewis bases such as THF,^{6,8} pyridine, or phosphines, or with protic reagents such as alcohols, phenols, thiols, selenols, tellurols,⁹ calixarenes,¹⁰ boronous acids,¹¹ secondary phosphines,¹² or silanols.¹³ Transamination reactions involving treatment of $M\{N(SiMe_3)_2\}_2$ with primary or secondary amines have not been extensively studied. Rare examples include the reaction of H_2NDipp ($Dipp = C_6H_3-2,6-Pr_2$) with $Mn\{N(SiMe_3)_2\}_2$ to

* To whom correspondence should be addressed. E-mail: pppower@ucdavis.edu.

[†] Department of Chemistry.

[‡] Department of Physics.

(1) Bürger, H.; Wannagat, U. *Monatsh. Chem.* **1963**, *94*, 1007.

(2) Bürger, H.; Wannagat, U. *Monatsh. Chem.* **1964**, *95*, 1099.

(3) Andersen, R. A.; Faegri, K.; Green, J. C.; Haaland, A.; Lappert, M. F.; Leung, W.-P.; Rypdal, K. *Inorg. Chem.* **1988**, *27*, 1782.

(4) Bradley, D. C.; Hursthouse, M. B.; Malik, K. M. A.; Moseler, R. *Transition Met. Chem. (London)* **1978**, *3*, 353.

(5) Murray, B. D.; Power, P. P. *Inorg. Chem.* **1984**, *23*, 4584.

(6) Olmstead, M. M.; Power, P. P.; Shoner, S. C. *Inorg. Chem.* **1991**, *30*, 2547.

(7) Bradley, D. C.; Fisher, K. J. *J. Am. Chem. Soc.* **1971**, *93*, 921.

(8) Bradley, D. C.; Hursthouse, M. B.; Ibrahim, A. A.; Malik, K. M. A.; Motevalli, M.; Moseler, R.; Powell, H.; Runnacles, J. D.; Sullivan, A. C. *Polyhedron* **1990**, *9*, 2959.

(9) Gindelberger, D. E.; Arnold, J. *Inorg. Chem.* **1993**, *32*, 5813.

(10) Olmstead, M. M.; Sigel, G. S.; Hope, H.; Xu, X.; Power, P. P. *J. Am. Chem. Soc.* **1985**, *107*, 8087.

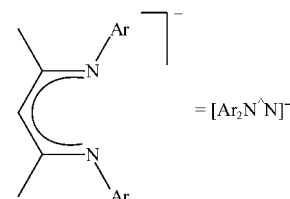
(11) Chen, H.; Power, P. P.; Shoner, S. C. *Inorg. Chem.* **1991**, *30*, 2884.

(12) Chen, H.; Olmstead, M. M.; Pestana, D. C.; Power, P. P. *Inorg. Chem.* **1991**, *30*, 1783.

(13) For a review see: Power, P. P. *Chemtracts: Inorg. Chem.* **1994**, *6*, 101.

give $\text{Mn}_3\{\mu\text{-N(H)Dipp}\}_4\{\text{N}(\text{SiMe}_3)_2\}_2^{14}$ and the reaction of $\text{Mn}\{\text{N}(\text{SiMe}_3)_2\}_2$ with the 1,2-diamine $\text{H}(\text{Dipp})\text{NCH}_2\text{CH}_2\text{N}(\text{Dipp})\text{H}$ to afford $\text{Mn}\{\text{N}(\text{Dipp})\text{CH}_2\text{CH}_2\text{N}(\text{Dipp})\text{H}\}_2^{15}$. The steric properties of the diprotic bidentate ligand $\text{H}(\text{Dipp})\text{NCH}_2\text{CH}_2\text{N}(\text{Dipp})\text{H}$ bear a resemblance to those of the monoprotic bidentate ligand $\text{H}(\text{Dipp})\text{NC}(\text{Me})\text{CHC}(\text{Me})\text{N}(\text{Dipp})$ which may be abbreviated as $\text{Dipp}_2\text{N}^{\wedge}\text{NH}$.¹⁶ This ligand and closely related ones have enjoyed considerable recent use in a variety of transition metal^{16–37} and main group complexes^{38–62} which have displayed a variety of stoichi-

ometries, low-coordination numbers, and bonding. In addition, they have been used as model species for the active sites in metalloenzymes^{28,29,31} and as catalysts for olefin polymerization.^{16,19,22–25,32,33,40,44} Very recent work has disclosed the preparation and characterization of the iron salts $(\text{Dipp}_2\text{N}^{\wedge}\text{N})\text{Fe}(\mu\text{-Cl})_2\text{Li}(\text{THF})_2$ and $\{(\text{Dipp}_2\text{N}^{\wedge}\text{N})\text{Fe}(\text{Cl})(\mu\text{-Cl})\}_2\text{Mg}(\text{THF})_2$ and the neutral species $(\text{Dipp}_2\text{N}^{\wedge}\text{N})\text{FeCl}$ in which three coordination has been achieved by increasing the steric properties of the β -diketiminato ligand via replacement of the methyl groups on the central C_3N_2 moiety by *tert*-butyl groups.⁶³ Moreover, reduction of the latter under N_2 has resulted in very interesting N_2 complexes of the type $(\text{Dipp}_2\text{N}^{\wedge}\text{N})\text{FeNNFe}(\text{N}^{\wedge}\text{NDipp}_2)'$ and $\text{K}_2(\text{Dipp}_2\text{N}^{\wedge}\text{N})\text{FeNNFe}(\text{N}^{\wedge}\text{NDipp}_2)'$.⁶⁴ It is now shown that reaction of $\text{Dipp}_2\text{N}^{\wedge}\text{NH}$ and related β -diketiminato ligands, as represented by the general formula



with the amides $\text{M}\{\text{N}(\text{SiMe}_3)_2\}_2$ ($\text{M} = \text{Mn}, \text{Fe}$ or Co) smoothly affords new β -diketiminates of the type $(\text{Ar}_2\text{N}^{\wedge}\text{N})\text{MN}(\text{SiMe}_3)_2$ where three coordination has been obtained with use of the bulky coligand $\text{N}(\text{SiMe}_3)_2$. In addition, it is shown that, in contrast to the reaction of $\text{LiN}^{\wedge}\text{NDipp}_2$ with FeCl_2 or CoCl_2 which afford “ate” complexes of the type $\text{Dipp}_2\text{N}^{\wedge}\text{NMC}_2\text{Li}(\text{THF})_2$ ($\text{M} = \text{Fe}^{63}$ or Co), reaction of $\text{LiN}^{\wedge}\text{NDipp}_2$ with FeCl_3 affords the neutral derivative $\text{Dipp}_2\text{N}^{\wedge}\text{NFeCl}_2$.

Experimental Section

General Procedures. All work was performed by using Schlenk techniques under an atmosphere of N_2 or in a Vacuum Atmospheres HE-43 drybox. All solvents were freshly distilled from Na/K and degassed three times immediately before use.

- (14) Kennepohl, D. K.; Brooker, S.; Sheldrick, G. M.; Roesky, H. W. *Z. Naturforsch* **1992**, *47B*, 9.
- (15) Chen, H.; Bartlett, R. A.; Dias, H. V. R.; Olmstead, M. M.; Power, P. P. *Inorg. Chem.* **1991**, *30*, 2487.
- (16) Feldman, J.; McLain, S. J.; Parthasarathy, A.; Marshall, W. J.; Calabrese, J. C.; Arthur, S. D. *Organometallics* **1997**, *16*, 1514.
- (17) Lappert, M. F.; Liu, D.-S. *J. Organomet. Chem.* **1995**, *500*, 203.
- (18) Rahim, M.; Taylor, N. J.; Xin, S.; Collins, S. *Organometallics* **1998**, *17*, 1315.
- (19) Gibson, V. C.; Maddox, P. J.; Newton, C.; Redshaw, C.; Solan, G. A.; White, A. J. P.; Williams, D. J. *Chem. Commun.* **1998**, 1651.
- (20) Budzelaar, P. H. M.; de Gelder, R.; Gal, A. W. *Organometallics* **1998**, *17*, 4121.
- (21) Kim, W.-K.; Fevola, M. J.; Liable-Sands, L. M.; Rheingold, A. L.; Theopold, K. H. *Organometallics* **1998**, *17*, 4541.
- (22) Budzelaar, P. H. M.; van Oort, A. B.; Orpen, A. G. *Eur. J. Inorg. Chem.* **1998**, 1485.
- (23) Budzelaar, P. H. M.; Moonen, N. N. P.; de Gelder, R.; Smits, J. M. M.; Gal, A. W. *Eur. J. Inorg. Chem.* **2000**, 753.
- (24) Cheng, M.; Lobkovsky, E. B.; Coates, G. W. *J. Am. Chem. Soc.* **1998**, *120*, 11018.
- (25) Lee, L. W. M.; Piers, W. E.; Elsegood, M. R. J.; Clegg, W.; Parvez, M. *Organometallics* **1999**, *18*, 2947.
- (26) Qian, B.; Scanlon, W. J.; Smith, M. R., III; Motry, D. H. *Organometallics* **1999**, *18*, 1693.
- (27) Kakaliou, L.; Scanlon, W. J., IV; Qian, B.; Baek, S. W.; Smith, M. R., III; Motry, D. H. *Inorg. Chem.* **1999**, *38*, 5964.
- (28) Holland, P. L.; Tolman, W. B. *J. Am. Chem. Soc.* **1999**, *121*, 7270.
- (29) Holland, P. L.; Tolman, W. B. *J. Am. Chem. Soc.* **2000**, *122*, 6331.
- (30) Prust, J.; Most, K.; Müller, I.; Stasch, A.; Roesky, H. W.; Usón, I. *Eur. J. Inorg. Chem.* **2001**, 1613.
- (31) Jazdzewski, B. A.; Holland, P. L.; Pink, M.; Young, V. G.; Spencer, D. J. E.; Tolman, W. B. *Inorg. Chem.* **2001**, *40*, 6097.
- (32) Hayes, P. G.; Piers, W. E.; Lee, L. W. M.; Knight, L. K.; Parvez, M.; Elsegood, M. R. J.; Clegg, W. *Organometallics* **2001**, *20*, 2533.
- (33) Gibson, V. C.; Newton, C.; Redshaw, C.; Solan, G. A.; White, A. J. P.; Williams, D. J. *Eur. J. Inorg. Chem.* **2001**, 1895.
- (34) Fehl, U.; Kaminsky, W.; Goldberg, K. *J. Am. Chem. Soc.* **2001**, *123*, 6423.
- (35) Yokota, S.; Tachi, Y.; Nishiwaki, M.; Ariga, M.; Itoh, S. *Inorg. Chem.* **2001**, *40*, 5316.
- (36) Hayes, P. G.; Piers, W.; McDonald, R. *J. Am. Chem. Soc.* **2002**, *124*, 2132.
- (37) Willems, S. T. H.; Budzelaar, P. H. M.; Moonen, N. N. P.; de Gelder, R.; Smits, J. M. M.; Gal, A. W. *Chem.—Eur. J.* **2002**, *8*, 1310.
- (38) Qian, B.; Ward, D. L.; Smith, M. R., III. *Organometallics* **1998**, *17*, 3070.
- (39) Cheng, M.; Darling, N. A.; Lobkovsky, E. B.; Coates, G. W. *Chem. Commun.* **1998**, 2007.
- (40) Radzewich, C. E.; Coles, M. P.; Jordan, R. F. *J. Am. Chem. Soc.* **1998**, *120*, 9384.
- (41) Kuchta, M. C.; Parkin, G. *New J. Chem.* **1998**, *22*, 523.
- (42) Clegg, W.; Cope, E. K.; Edwards, A. J.; Mair, F. S. *Inorg. Chem.* **1998**, *37*, 2317.
- (43) Rahim, M.; Taylor, N. J.; Xin, S.; Collins, S. *Organometallics* **1998**, *17*, 1315.
- (44) Radzewich, C. E.; Guzei, I. A.; Jordan, R. F. *J. Am. Chem. Soc.* **1999**, *121*, 8673.
- (45) Qian, B.; Baek, S. W.; Smith, M. R., III. *Polyhedron* **1999**, *18*, 2405.
- (46) Cui, C.; Roesky, H. W.; Hao, H.; Schmidt, H.-G.; Noltemeyer, M. *Angew. Chem., Int. Ed.* **2000**, *39*, 1815.
- (47) Bailey, P. J.; Dick, C. M. E.; Fabre, S.; Parsons, S. *Dalton* **2000**, 1655.
- (48) Gibson, V. C.; Segal, J. A.; White, A. J. P.; Williams, D. J. *J. Am. Chem. Soc.* **2000**, *122*, 7120.
- (49) Hardman, N. J.; Eichler, B. E.; Power, P. P. *Chem. Commun.* **2000**, 1491.
- (50) Cui, C.; Roesky, H. W.; Schmidt, H.-G.; Noltemeyer, M.; Hao, H.; Cimpoesu, F. *Angew. Chem., Int. Ed.* **2000**, *39*, 4274.
- (51) Ding, Y.; Roesky, H. W.; Noltemeyer, M.; Schmidt, H.-G.; Power, P. P. *Organometallics* **2001**, *20*, 1190.
- (52) Hardman, N. J.; Power, P. P. *Inorg. Chem.* **2001**, *40*, 2474.
- (53) Hardman, N. J.; Cui, C.; Roesky, H. W.; Fink, W. H.; Power, P. P. *Angew. Chem., Int. Ed.* **2001**, *40*, 2172.
- (54) Hardman, N. J.; Power, P. P. *Chem. Commun.* **2001**, 1184.
- (55) Hardman, N. J.; Power, P. P.; Gorden, J. D.; Macdonald, C. L. B.; Cowley, A. H. *Chem. Commun.* **2001**, 1866.
- (56) Stender, M.; Phillips, A. D.; Power, P. P. *Inorg. Chem.* **2001**, *40*, 5314.
- (57) Bailey, P. J.; Liddle, S. T.; Morrison, C. A.; Parsons, S. *Angew. Chem., Int. Ed.* **2001**, *40*, 4463.
- (58) Bailey, P. J.; Liddle, S. T.; Parsons, S. *Acta Crystallogr.* **2001**, *E57*, 0661.
- (59) Bailey, P. J.; Liddle, S. T.; Parsons, S. *Acta Crystallogr.* **2001**, *E57*, 0863.
- (60) Akkari, A.; Byrne, J. J.; Saur, I.; Rima, G.; Gornitzka, H.; Barrau, J. *J. Organomet. Chem.* **2001**, *622*, 190.
- (61) Stender, M.; Wright, R. J.; Eichler, B. E.; Prust, J.; Olmstead, M. M.; Roesky, H. W.; Power, P. P. *Dalton* **2001**, 3465.
- (62) Stender, M.; Eichler, B. E.; Hardman, N. J.; Power, P. P.; Prust, J.; Noltemeyer, M.; Roesky, H. W. *Inorg. Chem.* **2001**, *40*, 2799.
- (63) Smith, J. M.; Lachicotte, R. J.; Holland, P. L. *Chem. Commun.* **2001**, 1542.
- (64) Smith, J. M.; Lachicotte, R. J.; Pittard, K. A.; Cundari, T. R.; Lukat-Rodgers, G.; Rodgers, K. R.; Holland, P. L. *J. Am. Chem. Soc.* **2001**, *123*, 9222.

The compounds $M\{N(\text{SiMe}_3)_2\}_2$ [$M = \text{Mn},^1 \text{Fe},^2 \text{Co}^3$], $\text{Dipp}_2\text{N}^{\wedge}\text{NH}$,^{16,61} $\text{Mes}_2\text{N}^{\wedge}\text{NH}$,²² $(2,6\text{-Me}_2\text{C}_6\text{H}_3)_2\text{N}^{\wedge}\text{NH}$,²³ and $(2,6\text{-Cl}_2\text{C}_6\text{H}_3)_2\text{N}^{\wedge}\text{NH}$ ²³ were synthesized by literature methods. Anhydrous CoCl_2 (Aldrich), FeCl_3 (Aldrich), and 1.6 M *n*-BuLi in hexanes (Acros) were purchased from the commercial suppliers and were used without further purification. ¹H NMR spectra were recorded in C_6D_6 or CDCl_3 at 300 MHz on a QE-300 spectrometer. Infrared spectra were obtained as Nujol mulls with use of a Perkin-Elmer-1430 spectrometer. Electronic absorption spectra were obtained on a Hitachi U-2000 UV-vis spectrometer. Melting points are uncorrected and were determined for samples in capillaries sealed with grease. For magnetic measurements, the samples were sealed under vacuum in $3.2 \times 2 \text{ mm}^2$ quartz tubing. The sample holder was designed to minimize the background signal. The sample magnetization was measured using a Quantum Design MPMSXL7 superconducting quantum interference device (SQUID) magnetometer. For each measurement, the sample was zero-field cooled to 5 K, and the magnetization was measured as a function of field to 2 T. The field was then reduced to 1 T, and the magnetization of the sample was measured in 5 K increments to 300 K.

$(\text{C}_6\text{F}_5)_2\text{N}^{\wedge}\text{NH}$. A mixture of 2,3,4,5,6-pentafluoroaniline (8.0 g, 43.7 mmol), 2,4-pentanedione (1.9 g, 19.0 mmol), and *p*-toluenesulfonic acid (3.4 g, 18 mmol) in toluene (150 mL) was refluxed in a Dean-Stark apparatus for 24 h. The slurry was filtered to give a brown solid that was treated with 50 g of Na_2CO_3 in water (300 mL) and 300 mL of diethyl ether. The mixture was stirred for 45 min. The organic layer was isolated, dried with MgSO_4 , and filtered. The solvent was removed, and the product was washed with 50 mL of cold methanol. Yield: 4.8 g (59%), mp 66–68 °C. ¹H NMR (CDCl_3 , 300 MHz, 25 °C): δ 1.95 (s, 6H, CH_3), 5.20 (s, H, g-CH), 12.08 (s, H, NH). ¹³C{¹H} NMR (CDCl_3 , 75 MHz, 25 °C): δ 21.0 (CH_3), 99.2 (γ -C), 119.9 (*m*-C), 136.5 (*p*-C), 139.5 (*o*-C), 142.8 (*i*-C), 164.2 (CN). ¹⁹F{¹H} NMR (CDCl_3 , 376.12 MHz, 25 °C): δ -146.6 (m, 4F, *o*-F, ³J = 22.9 Hz, ⁴J = 6.1 Hz), -158.32 (t, 2F, *p*-F, ³J = 21.3 Hz), -160.78 (m, 4F, *m*-F, ³J = 21.3 Hz, ⁴J = 6.1 Hz).

$\text{Dipp}_2\text{N}^{\wedge}\text{NMnN}(\text{SiMe}_3)_2$ (1). A mixture of $\text{Mn}\{N(\text{SiMe}_3)_2\}_2$ (0.75 g, 2 mmol) and $\text{Dipp}_2\text{N}^{\wedge}\text{NH}$ (0.84 g, 2 mmol) in a Schlenk tube was heated at 110–120 °C under reduced pressure (ca. 0.03 mm) until bubbling had ceased (ca. 5 min). Upon cooling to room temperature, a dark yellow solid was obtained. This was dissolved in hexane (15 mL) and cooled in a ca. -20 °C freezer overnight to afford the product as yellow crystals. Yield: 0.55 g (43%), mp 235–237 °C. IR (Nujol, cm^{-1}): 2950, 2920, 2840, 1520, 1310, 1170, 1095, 1015, 930, 870, 750, 660, 400, and 350. UV-vis (hexane, λ_{max} , nm (ϵ , $\text{M}^{-1} \text{cm}^{-1}$): 231 (11 000), 376 (11 000), 443 (1040), and 466 (690). μ_{eff} : 5.65(3) μ_{B} .

$\text{Dipp}_2\text{N}^{\wedge}\text{NFeN}(\text{SiMe}_3)_2$ (2a). This was synthesized in a manner similar to the manganese derivative **1** with use of $\text{Dipp}_2\text{N}^{\wedge}\text{NH}$ (0.84 g, 2 mmol) and $\text{Fe}\{N(\text{SiMe}_3)_2\}_2$ (0.75 g, 2 mmol) and recrystallized as orange plates from hexane. Yield: 0.47 g (37%), mp 212–214 °C. IR (Nujol, cm^{-1}): 2920, 2850, 1520, 1315, 1170, 1100, 1020, 980, 875, 760, 670, and 355. UV-vis (hexane, λ_{max} , nm (ϵ , $\text{M}^{-1} \text{cm}^{-1}$): 318 (12 500), 371 (12 700), 483 (600), and 799 (600). μ_{eff} : 4.94(2) μ_{B} .

$(\text{C}_6\text{F}_5)_2\text{N}^{\wedge}\text{NFeN}(\text{SiMe}_3)_2$ (2b). The synthesis was accomplished in the same manner with use of $(\text{C}_6\text{F}_5)_2\text{N}^{\wedge}\text{NH}$ (0.81 g, 1.88 mmol) and $\text{Fe}\{N(\text{SiMe}_3)_2\}_2$ (0.75 g, 2 mmol) to afford the product as orange-yellow crystals. Yield: 0.75 g (62%), mp 108–110 °C. IR (Nujol, cm^{-1}): 2920, 2840, 1510, 1500, 1445, 1370, 1310, 1250, 1010, 990, 825, 670, 630, and 350.

$\text{Mes}_2\text{N}^{\wedge}\text{NFe}(\text{SiMe}_3)_2$ (2c). This was prepared in the same manner from $\text{Mes}_2\text{N}^{\wedge}\text{NH}$ (0.66 g, 2 mmol) and $\text{Fe}\{N(\text{SiMe}_3)_2\}_2$ (0.75 g, 2

mmol) to afford the product as orange crystals. Yield: 0.51 g (46%), mp 135–137 °C. IR (Nujol, cm^{-1}): 2920, 2860, 1610, 1460, 1380, 1260, 1100, 800, and 350. UV-vis (hexane, λ_{max} , nm (ϵ , $\text{M}^{-1} \text{cm}^{-1}$): 378 (12 400), 406 (11 100), 482 (3400), 779 (130), and 972 (250).

$(2,6\text{-Me}_2\text{C}_6\text{H}_3)_2\text{N}^{\wedge}\text{NFe}(\text{SiMe}_3)_2$ (2d). This was prepared in a manner similar to **2a** as orange crystals from $(2,6\text{-Me}_2\text{C}_6\text{H}_3)_2\text{N}^{\wedge}\text{NH}$ (0.60 g, 2 mmol) and $\text{Fe}\{N(\text{SiMe}_3)_2\}_2$ (0.75 g, 2 mmol). Yield: 0.49 g (47%), mp 88–90 °C. IR (Nujol, cm^{-1}): 2920, 2850, 1520, 1460, 1365, 1260, 1245, 1180, 1095, 1020, 970, 870, 760, 670, 350. UV-vis (hexane; λ_{max} , nm (ϵ , $\text{M}^{-1} \text{cm}^{-1}$): 376 (12 000), 404 (10 900), 480 (3 200), 776 (130), and 970 (230).

$(2,6\text{-Cl}_2\text{C}_6\text{H}_3)_2\text{N}^{\wedge}\text{NFe}(\text{SiMe}_3)_2$ (2e). This was synthesized in a manner similar to **2a** as orange crystals from $(2,6\text{-Cl}_2\text{C}_6\text{H}_3)_2\text{N}^{\wedge}\text{NH}$ (0.78 g, 2 mmol) and $\text{Fe}\{N(\text{SiMe}_3)_2\}_2$ (0.75 g, 2 mmol). Yield: 0.72 g (73%), mp 94–96 °C. IR (Nujol, cm^{-1}): 2920, 2840, 1525, 1435, 1370, 1255, 1195, 1150, 1020, 980, 930, 825, 675, and 365. UV-vis (hexane; λ_{max} , nm (ϵ , $\text{M}^{-1} \text{cm}^{-1}$): 362 (10 000), 411 (8100), 490 (2100), and 780 (110).

$\text{Dipp}_2\text{N}^{\wedge}\text{NCoN}(\text{SiMe}_3)_2$ (3). This was prepared in a manner similar to the manganese derivative **1** and isolated as red needles from hexane. Yield: 0.35 g (30%), mp 192–194 °C. IR (Nujol, cm^{-1}): 2920, 2840, 1525, 1315, 1175, 1095, 1020, 930, 870, 720, 660, 385, and 360. UV-vis (hexane; λ_{max} (ϵ , $\text{M}^{-1} \text{cm}^{-1}$): 235 (14 300), 316 (14 300), 437 (1230), 470 (670). μ_{eff} : 4.81(3) μ_{B} .

$\text{Fe}\{N^{\wedge}(\text{C}_6\text{F}_5)_2\}_2$ (4). This was obtained as red crystals from the mother liquor of **2b**. Yield: 0.70 g (38%), mp 206–208 °C. IR (Nujol, cm^{-1}): 2900(b), 2640, 2440, 1630, 1500, 1360, 1160, 1000, 765, 710, 700, 640, 530, 475, 330, and 300. UV-vis (hexane; λ_{max} (ϵ , $\text{M}^{-1} \text{cm}^{-1}$): 223 (8400), 338 (12 300), 437 (2900), 868 (230), 976 (140).

$\text{Dipp}_2\text{N}^{\wedge}\text{NCoCl}_2\text{Li}(\text{THF})_2$ (5). *n*-BuLi (6.2 mL of a 1.6 M solution in *n*-hexane) was added dropwise to a stirred solution of Dipp_2NNH (4.0 g, 9.5 mmol) in ca. 30 mL of diethyl ether with cooling in an ice bath. After overnight stirring, the solution of the $\text{Dipp}_2\text{N}^{\wedge}\text{NLi}$ was added dropwise to a suspension of CoCl_2 (1.24 g, 9.5 mmol) in THF (ca. 15 mL) with cooling in an ice bath. After overnight stirring, the color had changed to dark green. The solvents were removed under reduced pressure, and the residue was recrystallized from toluene (30 mL) as red crystals. Yield: 4.4 g (55%) IR (Nujol, cm^{-1}): 1520, 1460, 1315, 1260, 1175, 1100, 1040, 935, 890, 790, 755, 400, and 305. UV-vis (hexane; λ_{max} (ϵ , $\text{M}^{-1} \text{cm}^{-1}$): 250 (9200), 322 (9300), 432 (1900), 532 (1250), 615 (1100), and 868 (1150).

$\text{Dipp}_2\text{N}^{\wedge}\text{NFeCl}_2$ (6). The synthesis was accomplished with use of $\text{Dipp}_2\text{N}^{\wedge}\text{NLi}$ (9.5 mmol) and FeCl_3 (1.54 g, 9.5 mmol) in ca. 15 mL of toluene. Filtration and cooling in ca. -20 °C freezer afford green crystals of **6** that were suitable for X-ray crystallography. Yield: 2.75 g (53%), mp 202–204 °C. IR (Nujol, cm^{-1}): 1520, 1460, 1375, 1335, 1315, 1260, 1096, 1020, 930, 795, 755, 400, and 365. UV-vis (hexane; λ_{max} (ϵ , $\text{M}^{-1} \text{cm}^{-1}$): 319 (8200), 382 (8200), 553 (4600), and 813 (1800).

X-ray Crystallographic Studies. Crystals of **1–2d** and **3–6** were removed from the Schlenk tube under a stream of N_2 and immediately covered with a layer of hydrocarbon oil. A suitable crystal was selected, attached to a glass fiber, and quickly placed in the low-temperature nitrogen stream.⁶⁵ The data were recorded near 90 K (293 K for **6**) for a Bruker SMART 1000 (Mo $\text{K}\alpha$ radiation and a CCD area detector). The SHELXTL version 5.03 program package was used for the structure solutions and refinements.⁶⁶ Absorption corrections were applied using the SADABS program.⁶⁷ The crystal structures were solved by direct methods and refined by full-matrix least-squares procedures. All non-

Table 1. Data Collection Parameters for Compounds **1**, **2a–d**, **3–6**

	1	2a	2b	2c	2d	3	4	5	6
formula	C ₃₅ H ₅₉ Mn- N ₃ Si ₂	C ₃₅ H ₅₉ Fe- N ₃ Si ₂	C ₂₃ H ₂₅ F ₁₀ Fe- N ₃ Si ₂	C ₂₉ H ₄₇ Fe- N ₃ Si ₂	C ₂₇ H ₄₃ Fe- N ₃ Si ₂	C ₃₅ H ₅₉ Co- N ₃ Si ₂	C ₃₄ H ₁₄ F ₂₀ - FeN ₄	C _{47.5} H _{67.5} Cl ₂ - CoLiN ₂ O ₂	C ₂₉ H ₄₁ Cl ₂ - FeN ₂
fw	632.97	633.88	645.49	549.73	521.67	636.96	914.34	835.31	544.39
cryst syst	monoclinic	monoclinic	triclinic	monoclinic	monoclinic	monoclinic	triclinic	monoclinic	monoclinic
<i>a</i> (Å)	9.0944(6)	9.0729(5)	10.1239(5)	17.091(3)	20.321(2)	9.0909(5)	10.1625(4)	16.455(1)	12.5392(6)
<i>b</i> (Å)	20.232(1)	20.186(1)	13.8608(6)	15.102(3)	14.173(1)	20.199(1)	11.3316(4)	17.827(1)	19.5799(9)
<i>c</i> (Å)	20.278(1)	20.215(1)	21.041(1)	12.501(3)	20.577(2)	20.105(1)	15.9244(6)	15.830(1)	13.1323(6)
α (deg)			104.737(1)				100.059(1)		
β (deg)	90.053(2)	90.503(1)	90.050(1)	101.248(9)	96.404(5)	91.090(1)	95.239(1)	91.486(1)	117.136(1)
γ (deg)			100.889(2)				111.038(1)		
<i>V</i> (Å ³)	3731.3(4)	3702.1(3)	2800.4(2)	3164.5(11)	5927(1)	3691.4(1)	1673.5(1)	4642.2(5)	2869.3(2)
<i>Z</i>	4	4	4	4	8	4	2	4	4
μ (Mo K α) (mm ⁻¹)	0.444	0.498	0.709	0.573	0.608	0.556	0.597	1.195	1.260
<i>T</i> /K	90(2)	90(2)	90(2)	90(2)	91(2)	90(2)	90(2)	90(2)	293(2)
R1	0.0473	0.0349	0.0341	0.0302	0.0493	0.0342	0.0342	0.0394	0.0481
wR2	0.114	0.0933	0.0928	0.0867	0.1463	0.0864	0.0881	0.1047	0.1048

hydrogen atoms were refined anisotropically. Hydrogen atoms were included in the refinement at calculated positions using a riding model included in the SHELXTL program. Some details of the data collection and refinement are given in Table 1. Further details are provided in the Supporting Information.

Results and Discussion

Synthesis. The compounds that have been synthesized and characterized in this paper are indicated by the formulas Dipp₂N[^]NMnN(SiMe₃)₂, **1**; Dipp₂N[^]NFeN(SiMe₃)₂, **2a**; (C₆F₅)₂N[^]NFeN(SiMe₃)₂, **2b**; Mes₂N[^]NFeN(SiMe₃)₂, **2c**; (2,6-Me₂C₆H₃)₂N[^]NFeN(SiMe₃)₂, **2d**; (2,6-Cl₂C₆H₃)₂-N[^]NFeN(SiMe₃)₂, **2e**; Dipp₂N[^]NCoN(SiMe₃)₂, **3**; Fe{N[^]N-(C₆F₅)₂}₂, **4**; Dipp₂N[^]NCoCl₂Li(THF)₂, **5**; Dipp₂N[^]NFeCl₂, **6**, where the abbreviation N[^]N has been used to represent the central ring of the β -diketiminato ligand, as illustrated in the Introduction. The series of eight compounds **1–4** were obtained in a facile manner by the direct reaction of the Ar₂N[^]NH ligand with the metal amides M{N(SiMe₃)₂}₂ at ca. 100 °C in the absence of solvent. Purification was accomplished by recrystallization from hexane to give the products as air-sensitive crystals with nonoptimized yields in the range 40–70%. It was found during the preparation of pentafluorophenyl compound **2b** that both N(SiMe₃)₂ groups could be displaced from iron to give bis- β -diketiminato species **4**. The double substitution probably occurs as a result of the higher acidity of (C₆F₅)₂N[^]NH and the fact that it is the least sterically crowding of the β -diketiminato ligands used in this work. There was no evidence for a bis-(diketiminato) product in any of the reactions with the bulkier Dipp₂N[^]NH ligand. The lack of a doubly substituted product may be contrasted with the reaction between the sterically related diamine H(Dipp)NCH₂CH₂(Dipp)H and Mn{N(SiMe₃)₂}₂ which afforded the unusual disubstituted species Mn{N(Dipp)CH₂CH₂N(Dipp)H}₂.¹⁵ The reaction of LiN[^]NDipp₂ with CoCl₂ in the hexane/ether/THF solvent mixture afforded the “ate” product **5** as red crystals. This result is similar to the previously reported synthesis of the iron compound Dipp₂N[^]NFeCl₂Li(THF)₂ which also crystallizes as an “ate” complex.⁶³ Seemingly, the combination of Dipp₂N[^]N and a single chloride ligand in the putative species

Dipp₂N[^]NMCl (M = Fe or Co) is insufficiently crowding to prevent association with another chloride. However, it has been shown that when Dipp₂N[^]N ligand was modified by replacement of the methyls on the ligand backbone with *tert*-butyl groups (designated (Dipp₂N[^]N)') the neutral species (Dipp₂N[^]N)'

FeCl was obtained in which lithium chloride was eliminated and the iron is bound only to the β -diketiminato ligand and a chloride to yield a three-coordinate metal environment.⁶³ Direct reaction of Dipp₂N[^]NLi with FeCl₃ in toluene afforded the neutral Fe³⁺ compound Dipp₂N[^]NFeCl₂, **6**, as green crystals in ca. 50% yield. No problems were encountered with the separation of LiCl, probably as a result of the more crowded, higher coordinate, character of the iron.

Spectroscopic and Magnetic Studies

The magnetic moments of the compounds were measured in C₆D₆ solution by the Evans' method. These measurements afforded $\mu_{\text{eff}}(\text{C}_6\text{D}_6)$ values that were consistent with high spin d⁵ (**1**, $\mu_{\text{B}} = 5.9(1)$; **6**, $\mu_{\text{B}} = 5.9(1)$), d⁶ (**2a–e** and **4**, $\mu_{\text{B}} = 4.9–5.1(1)$), and d⁷ (**3**, $\mu_{\text{B}} = 4.9(1)$; **5**, $\mu_{\text{B}} = 5.0(1)$) configurations that have five, four, and three unpaired electrons, respectively. Magnetic studies of crystalline samples of **1**, **2a**, and **3** were also undertaken. Plots of $1/\chi$ versus temperature in the range 5–300 K afforded linear or near linear relationships. The compounds displayed the expected Curie–Weiss behavior and afforded μ_{eff} values of 5.65(3) μ_{B} (**1**), 4.94(2) μ_{B} (**2a**), and 4.81(3) μ_{B} (**3**). These values are slightly lower than the solution values in the case of **1** and **3**. The reasons for these differences are unclear.

The presence of unpaired electrons in all the compounds gives rise to paramagnetically shifted ¹H NMR spectra. The spectra of the iron compounds **2a–e** (Table 2), which differ only in their nitrogen substituents, can be assigned as a result of the effects of the differences in substitution on the signals. The simplest ¹H NMR spectrum arises from C₆F₅ substituted species **2b** which has only three types of magnetically inequivalent hydrogens. In C₆D₆ at 25 °C, three major broadened signals were observed at δ –9.58, 50.84, and 93.45. In addition, a minor signal at –66.50 ppm was observed. The three major signals can be assigned to β -Me (δ –9.58), N(SiMe₃)₂ (δ 50.84), and γ -H (δ 93.45). Their

(65) Hope, H. *Prog. Inorg. Chem.* **1995**, *41*, 1.

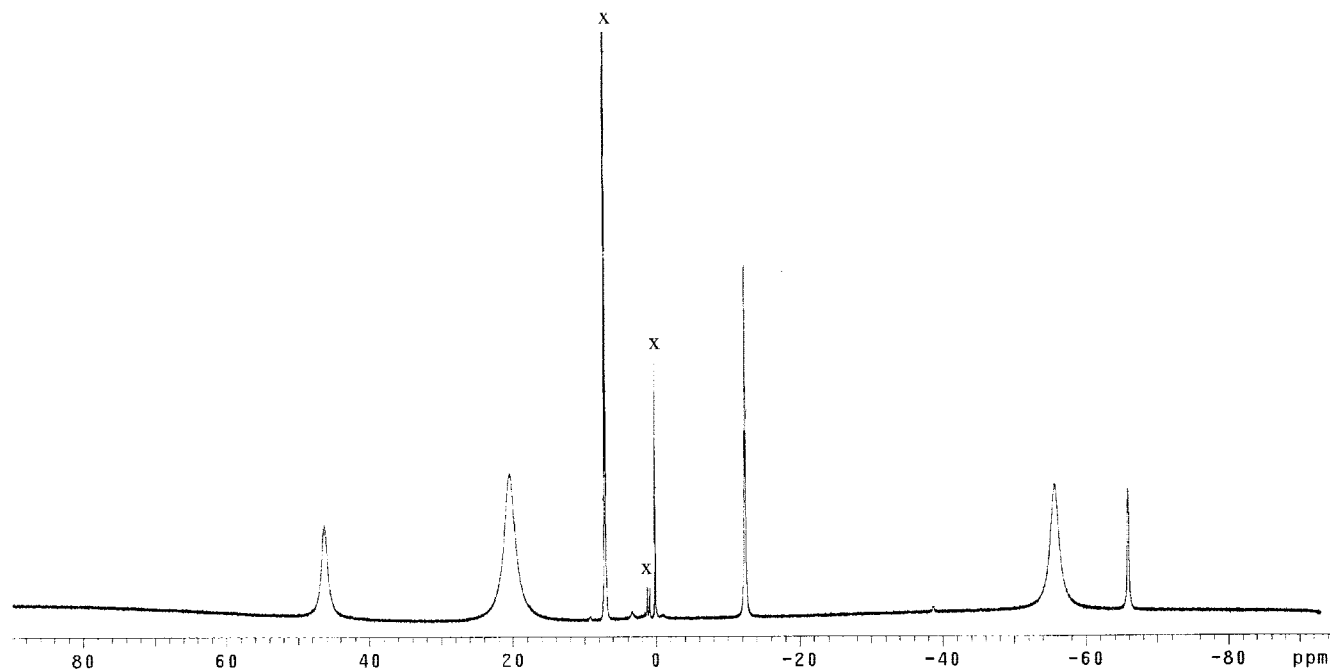


Figure 1. ^1H NMR spectrum of $(2,6\text{-Me}_2\text{H}_3\text{C}_6)_2\text{N}^{\wedge}\text{NFeN}(\text{SiMe}_3)_2$ (**2d**) in C_6D_6 at $25\text{ }^\circ\text{C}$. Solvent and free ligand peaks are marked x.

Table 2. ^1H NMR Shifts (ppm) of the Iron Compounds $\text{Ar}_2\text{N}^{\wedge}\text{NFeN}(\text{SiMe}_3)_2$, **2a–e** in C_6D_6 at ca. 298 K

	Ar	γ -H	β -Me	$\text{N}(\text{SiMe}_3)_2$	<i>o</i> -R	<i>m</i> -H	<i>p</i> -H(R)
2a	$\text{C}_6\text{H}_3\text{-2,6-Pr}_2$	83.2	-9.2	13.6	3.2, -44.1	51.6	-52.8
2b	C_6F_5	93.45	-9.58	50.84			
2c	$\text{C}_6\text{H}_2\text{-2,4,6-Me}_3$		-12.41	19.44	-55.41	48.01	27.2 (Me)
2d	$\text{C}_6\text{H}_3\text{-2,6-Me}_2$		-12.51	20.35	-55.91	46.24	-65.92
2e	$\text{C}_6\text{H}_3\text{-2,6-Cl}_2$	93.73	-9.46	30.34		9.13	-67.99

integration corresponded to the ratio of β -Me (6), $\text{N}(\text{SiMe}_3)_2$ (18), and γ -H (1) hydrogens present in the complex. The minor signal at δ -66.50 may be due to a small amount of bis- β -diketiminato complex **4** which is a byproduct of the reaction. The assignment of the δ 50.84 signal to the $\text{N}(\text{SiMe}_3)_2$ hydrogens is also supported by the similarity of the shift value to the δ 63.5 signal observed for monomeric $\text{Fe}\{\text{N}(\text{SiMe}_3)_2\}_2$ ⁷ and the methyl signals in the related monomeric complexes $\text{Fe}\{\text{N}(\text{SiMe}_2\text{Ph})_2\}_2$ (δ 49.9) and $\text{Fe}\{\text{N}(\text{SiMePh}_2)_2\}_2$ (δ 57.6).⁶⁸ A change in the aryl substituents at nitrogen from C_6F_5 (**2b**) to $\text{C}_6\text{H}_3\text{-2,6-Cl}_2$ (**2e**) should result in two new hydrogen signals (i.e., of the meta and para hydrogens), and this is what is observed. The signals in the spectrum of **2e** due to $\text{N}(\text{SiMe}_3)_2$ (δ 30.34), β -Me (δ -9.46), and γ -H (δ 93.73) are readily assignable. The new signals appear at δ 9.13 and δ -67.99. These are assignable to the meta and para hydrogens. They integrate in a 2:1 ratio and in the correct intensity relative to the $\text{N}(\text{SiMe}_3)_2$ and β -Me signals. Replacement of the chlorines in **2e** with methyl groups affords **2d** whose ^1H NMR spectrum is shown in Figure 1. The β -Me (δ -12.51) and $\text{N}(\text{SiMe}_3)_2$ (δ 20.35) signals of **2d** are shifted slightly upfield in comparison with

those of **2e**. The *p*-H signal (δ -65.92) is very close to that in **2e** but the *m*-H signal is observed at δ 46.24. The new signal at δ -55.91 is attributable to the *o*-Me hydrogens. No signal readily assignable to γ -H could be observed. The mesityl substituted **2c** differs from **2d** at the para positions only. Thus, the chemical shifts of β -Me, $\text{N}(\text{SiMe}_3)_2$, *o*-Me, and *m*-H of **2c** are very similar to those observed in **2d**. The *p*-H signal seen at δ -65.92 in **2d** is not observed in **2c**. Instead, a new, more intense, narrow signal at δ 27.2, attributable to the *p*-Me of the mesityl groups, is observed. Finally, in **2a**, the resonances at δ -9.2 and δ 13.6 are assignable to the β -Me hydrogens and $\text{N}(\text{SiMe}_3)_2$ groups, and the signal at δ 51.6 is due to the *m*-Hs. These values are similar to those observed in **2c** and **2d**. Assignments of further peaks at δ -52.8 and δ 83.2 to the *p*-H and γ -H signals seem reasonable in view of their similarity to the corresponding signals in **2b**, **2d**, and **2e**. The assignment of the signals associated with the Pr^i substituents is more complicated because the methyl groups are diastereotopic, and two equally intense resonances which integrate in the ratio 12H each (when their intensity is compared to the $\text{N}(\text{SiMe}_3)_2$ and β -Me signals) were observed at δ 3.2 and -44.1.

The electronic spectra of **1–6** are characterized by intense absorptions (ϵ values as high as 14 000) at wavelengths generally shorter than 380 nm that are attributable to π - π^* transitions of the β -diketiminato and aryl substituents or metal- β -diketiminato charge transfer transitions. These intense peaks tail into the visible region, and this feature is probably responsible for the prevalence of the yellow to red color of the majority of the complexes. Less intense absorptions are observed at longer wavelengths, and those that occur at ca. <500 nm are usually shoulder features on the more intense π - π^* absorption at shorter wavelengths. The spectra of the iron complexes **2a–e** feature two

(66) SHELXL, version 5.1; Bruker AXS: Madison, WI.

(67) SADABS an empirical absorption correction program, part of the SAINTPlus NT version 5.0 package; Bruker AXS: Madison, WI, 1998.

(68) Chen, H.; Bartlett, R. A.; Dias, H. v. R.; Olmstead, M. M.; Power, P. P. *J. Am. Chem. Soc.* **1989**, *111*, 4338.

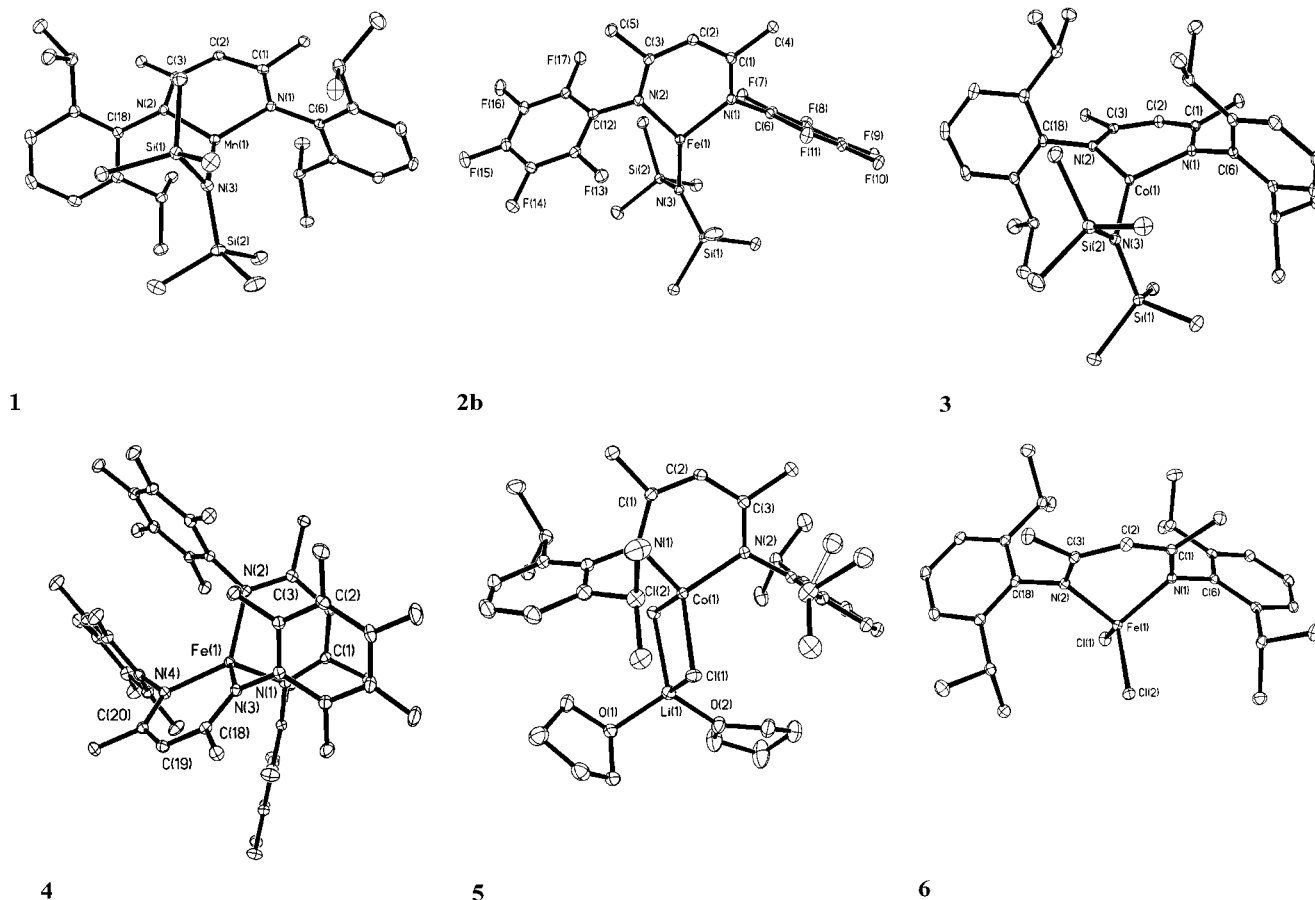


Figure 2. Illustrations (30% thermal ellipsoids) of the structures of $\text{Dipp}_2\text{N}^\wedge\text{NMnN}(\text{SiMe}_3)_2$ (**1**), $(\text{C}_6\text{F}_5)_2\text{N}^\wedge\text{NFeN}(\text{SiMe}_3)_2$ (**2b**), $\text{Dipp}_2\text{N}^\wedge\text{NCoN}(\text{SiMe}_3)_2$ (**3**), $\text{Fe}\{\text{N}^\wedge\text{N}(\text{C}_6\text{F}_5)_2\}_2$ (**4**), $\text{Dipp}_2\text{N}^\wedge\text{NCoCl}_2\text{Li}(\text{THF})_2$ (**5**), and $\text{Dipp}_2\text{N}^\wedge\text{NFeCl}_2$ (**6**). H atoms are not shown. Selected bond distances and angles are in Table 3.

prominent absorptions in the ranges 480–490 nm and 775–790 nm with a shoulder feature at ca. 400 nm visible for **2c**, **2d**, and **2e**. A weak band at ca. 970 nm in **2c** and **2d** is also apparent. The ground state of the free ion $\text{Fe}^{2+}(\text{d}^6)$ term is ^5D , and this is expected to split into $^5\text{A}' + ^5\text{E}' + ^5\text{E}''$ terms in a trigonal planar (D_{3h}) field so that at least two d–d transitions are expected. However, the geometric distortions due to the β -diketiminato ligand lower the local symmetry at the metal further to C_{2v} . Thus, the E bands could be further split which, if great enough, could give rise to further absorptions. However, the spectra of **2a** suggest that this splitting is not large.

Structures

All compounds except **2e** were characterized by X-ray crystallography. Six of these nine structures, that is, **1**, **2a–d**, and **3**, are related in that they feature the metal bound to one β -diketiminato and one $\text{N}(\text{SiMe}_3)_2$ ligand. Representative structures are shown in Figure 2. Selected bond lengths and angles are given in Table 3. They display an essentially planar, three-coordinate^{69–72} geometry at the metals. How-

ever, there are very marked deviations of the interligand angles from 120° . The narrowest angle in each complex is associated with the β -diketiminato ligand where the $\text{N}(1)\text{—M—N}(2)$ angles are in the range $92.57(6)\text{—}96.60(4)^\circ$. The remaining interligand angles are wider and span the range $126.98(5)\text{—}139.76(5)^\circ$. Another notable structural distortion concerns the MN_2C_3 ring geometries which display folding along the $\text{N}(1)\cdots\text{N}(2)$ line in the case of **1**, **2a**, and **3** (fold angles = ca. 165°) but are much closer to planarity for **2b**, **2c**, and **2d**. It is noteworthy that the greatest folding is observed in the derivatives of the bulkiest $\text{Dipp}_2\text{N}^\wedge\text{N}$ ligand (i.e., complexes **1**, **2a**, and **3**) and this finding is consistent with previous structural studies of other metal complexes of this ligand where folding was attributed to the steric requirements of the *Dipp* substituents.⁶² Within the β -diketiminato rings, the N_2C_3 moiety is planar, and the N—C and C—C distances lie in the narrow ranges $1.328(2)\text{—}1.347(2)$ Å and $1.396(3)\text{—}1.416(2)$ Å consistent with the multiple character of these bonds. The internal angles within the rings display little variation across the series. In each complex, the widest angle is observed at $\text{C}(2)$ which has an average value of $129.3(4)^\circ$. The angle in each complex is within ca. 0.6° of this value. The M—N bonds to the β -diketiminato ligands are ca. $0.05\text{—}0.10$ Å longer than those to the $\text{N}(\text{SiMe}_3)_2$ groups. This is consistent with their semidative character. The compounds **1**, **2a**, and **3** have the same ligand

(69) Bradley, D. C. *Chem. Ber.* **1975**, *11*, 393.

(70) Eller, P. G.; Bradley, D. C.; Hursthouse, M. B.; Meek, D. W. *Coord. Chem. Rev.* **1987**, *24*, 1.

(71) Cummins, C. C. *Prog. Inorg. Chem.* **1998**, *47*, 685.

(72) Alvarez, S. *Coord. Chem. Rev.* **1999**, *193–195*, 13.

Table 3. Selected Bond Distances (Å) and Angles (deg) for **1–5**

	1	2a	3
M–N(1)	2.050(1)	2.027(1)	1.982(1)
M–N(2)	2.096(1)	1.988(1)	1.947(1)
M–N(3)	1.992(1)	1.928(1)	1.903(1)
N(1)–M–N(2)	92.57(5)	94.33(4)	96.60(4)
N(1)–M–N(3)	135.81(6)	131.07(4)	129.03(4)
N(2)–M–N(3)	131.54(6)	134.39(4)	132.83(4)
M–N(1)–C(6)	118.98(10)	116.96(7)	118.20(8)
M–N(2)–C(18)	116.66(10)	118.95(7)	119.39(8)
N(1)–C(1)	1.342(2)	1.328(2)	1.330(2)
N(2)–C(3)	1.325(2)	1.340(2)	1.339(2)
C(1)–C(2)	1.398(2)	1.410(2)	1.411(2)
C(2)–C(3)	1.416(2)	1.400(2)	1.396(2)
N(3)–Si(1)	1.707(2)	1.716(1)	1.713(1)
N(3)–Si(2)	1.709(2)	1.718(1)	1.721(1)
M–N(3)–Si(1)	109.95(8)	111.77(5)	114.72(6)
M–N(3)–Si(2)	121.88(8)	121.58(6)	125.49(6)
Si(2)–N(3)–Si(3)	127.12(8)	125.50(6)	125.49(6)
fold angle/metal distance from N ₂ C ₃ plane	164.2/0.394	164.8/0.365	165.3/0.340
	2b	2c	2d
M–N(1)	2.008(1)	1.9969(9)	1.999(2)
M–N(2)	1.993(1)		1.990(2)
M–N(3)	1.908(1)	1.915(1)	1.917(2)
N(1)–M–N(2)	93.20(5)	95.73(5)	94.23(8)
N(1)–M–N(3)	126.98(5)	132.13(3)	129.79(8)
N(2)–M–N(3)	139.76(5)		135.88(8)
M–N(1)–C(2)	116.20(10)	118.90(7)	118.3(2)
M–N(1)–C(2)	116.38(10)		121.2(2)
N(1)–C(2)	1.341(2)	1.338(1)	1.331(3)
N(2)–C(2)	1.347(2)		1.346(3)
C(1)–C(2)	1.399(2)	1.404(1)	1.408(3)
C(2)–C(3)	1.401(2)		1.396(3)
N(3)–Si(1)	1.718(1)	1.7221(7)	1.726(2)
N(3)–Si(2)	1.716(1)		1.714(2)
M–N(3)–Si(1)	114.81(7)	118.51(4)	114.5(1)
M–N(3)–Si(2)	115.52(7)		120.2(1)
Si(2)–N(3)–Si(3)	129.31(8)	122.98(8)	124.7(1)
fold angle/metal distance from N ₂ C ₃ plane	178.6/0.028	178.4/0.031	157.3/0.556 177.8/0.039
	4	5	6
M(1)–N(1)	2.038(1)	1.963(2)	1.978(2)
M(1)–N(2)	2.013(1)	1.957(2)	1.951(2)
M(1)–N(3)	2.016(1)		
M(1)–N(4)	1.999(1)		
M(1)–Cl(1)		2.2933(6)	2.1852(6)
M(2)–Cl(2)		2.2955(6)	2.2106(6)
N(1)–C(1)	1.337(2)	1.336(3)	1.331(3)
N(2)–C(3)	1.343(2)	1.3349(3)	1.343(3)
N(3)–C(18)	1.334(2)		
N(4)–C(20)	1.350(2)		
C(1)–C(2)		1.405(3)	1.415(3)
C(2)–C(3)		1.402(6)	1.401(3)
N(1)–Fe(1)–N(2)	89.52(5)	98.23(8)	95.57(7)
N(3)–Fe(1)–N(4)	92.67(5)		
N(1)–Fe(1)–N(4)	121.00(5)		
N(2)–Fe(1)–N(3)	118.54(5)		
Fe(1)–N(1)–C(6)	119.72(9)	119.03(14)	121.51(1)
Fe(1)–N(2)–C(12)	120.68(9)	118.601(4)	
Fe(1)–N(2)–C(18)			124.9(1)
Cl(1)–Fe(1)–Cl(2)		100.18(2)	117.15(3)
fold angle/metal distance from N ₂ C ₃ plane	144.0/0.305 168.3/0.098	166.0/0.317	143.5/0.797

set (isoleptic), and the M–N bond lengths are in the sequence Mn–N > Fe–N > Co–N which is consistent with the decreasing size of the M²⁺ ions.⁷⁴ The M–N(SiMe₃)₂ distances are very similar to the terminal M–N bond lengths

in the neutral M(II) dimers [M{N(SiMe₃)₂}₂]₂^{4–6} which also feature three-coordinate metals. However, they are up to ca. 0.08 Å longer than the M–N distances in the three-coordinate, M(II) anions [M{N(SiMe₃)₂}₃][–].⁷³ The longer M–N distances in the latter are probably a result of increased interelectronic repulsion due to the presence of negative charge from the “extra” electron. The terminal MNSi₂ moieties in **1**, **2**, and **3** have planar geometries (as they have in all the structures), and they are oriented at angles of ca. 74° with respect to the MN₃ coordination planes.

The structures of the series of four iron derivatives **2a–d** also display interesting trends. The Fe–N (*β*-diketiminato) bond lengths are all within 0.01 Å of each other and have an average value of 2.000(9) Å. This is significantly longer than the 1.948(2) Å reported for (Dipp₂N[^]N)FeCl (in which the Me groups on the core ring are replaced by Bu^t groups).⁶³ Seemingly, the electronegative chloride ligand in the latter complex decreases the effective ionic radius of iron. This, together with the relatively small size of Cl, which relieves steric crowding, results in shorter Fe–N bonds. The trend for the Fe–N(SiMe₃)₂ bond lengths in **2a–d** lends support to the importance of steric effects. The longest distance, 1.928(1) Å, is observed for the bulkiest Dipp₂N[^]N derivative, **2a**, whereas the shortest distance, 1.908(1) Å, is seen with the least bulky (C₆F₅)₂N[^]N complex, **2b**. The essentially equal intermediate distances of 1.915(1) and 1.917(2) Å are observed with the Mes₂N[^]N and 2,6-Me₂C₆H₃N[^]N derivatives **2c** and **2d** which have almost identical steric properties near the iron and sizes between the extremes of **2a** and **2d**. In essence, the observed trend suggests that the bond length variations in these complexes are mainly a result of steric effects. However, electronic effects may also play a role because the widest Si–N–Si angle (129.31(3)°) corresponds to the shortest Fe–NSi₂ bond in the least crowded **2b**, which suggests that greater charge separation occurs across the Fe–NSi₂ bond. In addition, the torsion angles between FeNSi₂ and FeN₃ do not display a regular pattern. Thus, **2b**, the least sterically crowded molecule in the series, has an average torsion angle of 71.8° whereas the bulkier mesityl substituted **2c** has a torsion angle of 52.3° and the sterically very similar **2d** has a torsion angle of 85.0°.

The three compounds **4**, **5**, and **6** are also illustrated in Figure 2. The structure of **4** shows that iron is bound to two *β*-diketiminato ligands to afford an FeN₄ array that approximates *D*_{2d} symmetry with an average Fe–N distance of 2.017(11) Å. However, this averaged distance obscures the fact that for each *β*-diketiminato ligand one of the Fe–N distances is ca. 0.02 Å longer than the other, for example, Fe–N(1),N(2) = 2.038(1), 2.013(1) Å. The origin of this difference is uncertain, and it could be due to several factors among which are the unequal occupancy of d_{x²–y²} and d_{z²} orbitals of a d⁶ electron configuration in an approximately tetrahedral crystal field and crystal packing effects. The Fe–N distances in **4** are on average longer than the Fe–N(*β*-diketiminato) distances in **2b**, **2c**, and **2d** but are

(73) Putzer, M. A.; Neumuller, B.; Dehnicke, K.; Magull, J. *Chem. Ber.* **1996**, *129*, 715.

(74) Shannon, R. D. *Acta Crystallogr.* **1976**, *A32*, 751.

similar to those in **2a**. The lengthening in **4** is consistent with the higher coordination number of iron in this complex. The greater steric crowding in **2a** apparently eliminates the difference so that very similar distances are observed. Both β -diketiminato rings display folding, but the amount of folding in each ring is quite different. For the ring associated with N(1) and N(2), the fold angle is 154.0° , and the iron is 0.305 \AA out of the N_2C_3 plane. For the N(3) and N(4) ring, the angle is 168.3° , and the deviation is 0.098 \AA .

Cobalt species **5** crystallizes with 1.5 toluene molecules per asymmetric unit. The cobalt is bound to two β -diketiminato nitrogens and also to two chlorides which act as bridges to lithium. The lithium is further complexed by two THF oxygens. Thus, both metals have distorted tetrahedral coordination. The structure is similar to that of recently reported iron complex $\text{Dipp}_2\text{N}^{\wedge}\text{NFeCl}_2\text{Li}(\text{THF})_2$.⁶³ The Co–N and Co–Cl bonds, av $1.960(3)$ and $2.294(1) \text{ \AA}$, are shorter by ca. 0.04 \AA than the corresponding Fe–N and Fe–Cl distances in the iron species which is in keeping with the smaller effective ionic radius of Co^{2+} relative to Fe^{2+} .⁷⁴ As in the iron complex, the narrowest interligand angle in the Co^{2+} coordination sphere involves the β -diketiminato ligand ($98.23(8)^\circ$). The Li–Cl and Li–O distances $2.340(4)$ and $1.90(1) \text{ \AA}$ are also similar to those seen in the iron complex.

Iron(III) complex **6** is monomeric and features the metal in distorted tetrahedral coordination with Fe–N distances that are ca. 0.03 \AA shorter than those in compounds **2a–d**. This is unexpected on the basis of the higher iron coordination number but is in agreement with the higher oxidation state of iron in **6**. In contrast, the average Fe–Cl distance,

ca. 2.20 \AA , in **6** is longer than the $2.172(7) \text{ \AA}$ observed in $(\text{Dipp}_2\text{N}^{\wedge}\text{N})'\text{FeCl}$ which is in agreement with the higher iron coordination number but not its higher oxidation state.⁶³ The structure of **6** may be compared with those recently reported for $\text{Dipp}_2\text{N}^{\wedge}\text{NVCl}_2$ ²² and the group 13 derivatives $\text{Dipp}_2\text{N}^{\wedge}\text{-NMCl}_2$ ($M = \text{Al, Ga, or In}$).⁶² The structural parameters for **6** and $\text{Dipp}_2\text{N}^{\wedge}\text{NGaCl}_2$ are particularly close although the compounds are not isomorphous. However, the distortions in **6** are greater than those in the $\text{DippN}^{\wedge}\text{N}$ group 13 metal halide derivatives; the iron lies 0.797 \AA out of the averaged core N_2C_3 plane, and there is an angle of 143.5° between the FeN_2 and N_2C_3 planes. In sharp contrast to the monomeric formulas of **6** and its vanadium analogue,²² the recently reported chromium derivative $\{\text{Dipp}_2\text{N}^{\wedge}\text{NCr}(\text{Cl})(\mu\text{-Cl})\}_2$ is dimeric.³³ The reasons for the differences in association for the complexes are not obvious. The structure of **6** also resembles those of the more crowded $(\text{Dipp}_2\text{N}^{\wedge}\text{N})'\text{ScCl}_2$ ³² and $(\text{Dipp}_2\text{N}^{\wedge}\text{N})'\text{TiCl}_2$ ²² complexes in which the methyl substituents on the β -diketiminato ring are replaced by tertiary butyl groups.

Acknowledgment. We are grateful to the donors of the Petroleum Research Fund administered by the American Chemical Society and UC MEXUS-CONACYT and the Alexander von Humboldt Stiftung for the award of a fellowship to P.P.P.

Supporting Information Available: X-ray file in CIF format. This material is available free of charge via the Internet at <http://pubs.acs.org>.

IC025552S